

Topological defects in non-reciprocal active solids with odd elasticity

Lara Braverman,^{1,2,*} Colin Scheibner,^{1,2,*} and Vincenzo Vitelli^{1,2,3,†}

¹James Franck Institute, The University of Chicago, Chicago, Illinois 60637, USA

²Department of Physics, The University of Chicago, Chicago, Illinois 60637, USA

³Kadanoff Center for Theoretical Physics, The University of Chicago, Chicago, Illinois 60637, USA

In this Letter, we present the continuum theory of topological defects in active solids whose linear elasticity violates Maxwell-Betti reciprocity: the symmetry between mechanical perturbations and response. Such solids display odd elasticity, i.e. elastic moduli that do not arise from an elastic potential energy. Analytical calculations corroborated by numerical simulations of microscopic models reveal chiral strains and stresses induced by disclinations, dislocations, and point defects. The forces between dislocation pairs need not be reciprocal and can even alter their mechanical stability, paving the way for active generalizations of plasticity and defect-mediated melting.

Topological defects are local singularities in an order parameter that have global consequences for the behavior of many-body systems [1–6]. When combined with activity, i.e. microscopic sources of energy, defects give rise to a rich and varied phenomenology. Prominent examples include active nematic liquid crystals [7–12], active hexatics [13], and active inclusions in passive media [14–16]. Yet, the continuum mechanics of topological defects in active crystalline solids with non-conservative interactions is largely unexplored. In particular, we lack a mathematical treatment of the elastic distortions and interactions characterizing crystalline defects on par with their passive counterparts [17]. This would be a key step towards understanding phenomena such as active plasticity and defect-mediated melting that remain elusive [18–25].

Violations of reciprocity relations, such as Maxwell-Betti [26, 27], Onsager [28, 29] and Newton’s third law, are ubiquitous in active and biological systems as well as metamaterials [30–59]. However, the traditional theory of crystalline defects, inspired by metals [60–62] and shells [63–65], is built upon the crucial assumption that Maxwell-Betti reciprocity holds [1, 2, 17]. Qualitatively, Maxwell-Betti reciprocity is the symmetry between perturbation and response. In linear elasticity, it is equivalent to the existence of an elastic potential energy. Broken Maxwell-Betti reciprocity in continuum elastic media leads to additional elastic moduli captured by a framework called odd elasticity [66–70].

In this Letter, we start from the constitutive equations of odd elasticity and develop a systematic mechanical treatment of crystalline topological defects and their interactions in linear elastic media with broken Maxwell-Betti reciprocity. Our analytical calculations corroborated by numerical simulations of illustrative microscopic models reveal chiral contributions to the stress and strain fields of disclinations, dislocations and point defects, see Fig. 1. This chirality originates directly from the presence of odd elastic moduli that necessarily entail rota-

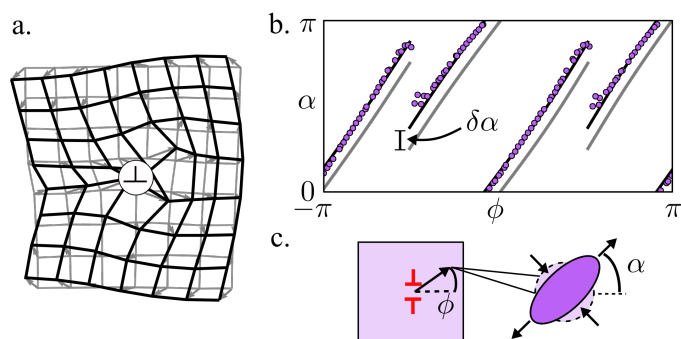


FIG. 1. Chiral strain distribution around defects in odd elastic solids. **a.** A chiral modification to the strain field of a dislocation induced by non-reciprocity. The black (grey) lines are deformed contours in a nonreciprocal (reciprocal) solid. **b-c.** Using a non-reciprocal mass-spring model described in the S.I., we numerically simulate the relaxation of a nonreciprocal microscopic lattice and compute the strain field around two pinned, anti-aligned dislocations. The orientation of the local shear strain is captured by an angle α , plotted as a function of the polar angle ϕ . The grey lines are theoretical curves for $\nu^o = 0$, the black lines (colored points) are theoretical curves (numerical data) for $\nu^o = -0.88$. See Fig. S2 for additional information.

tions in strain space for 2D isotropic media [66]. Moreover, we find that the forces between dislocation pairs need not be equal and opposite and can even affect the mechanical stability of defect configurations.

Elasticity without Maxwell-Betti reciprocity— The starting point of our analysis is that the work per unit area required to deform a solid is given by $\delta w(\mathbf{r}) = \sigma_{ij}(\mathbf{r})\delta u_{ij}(\mathbf{r})$ where $u_{ij}(\mathbf{r}) = \partial_i u_j(\mathbf{r})$ denotes gradients of displacement and $\sigma_{ij}(\mathbf{r})$ is the stress tensor. For small deformations, the stress-strain relationship of an elastic medium may be linearized, yielding $\sigma_{ij}(\mathbf{r}) = C_{ijkl}u_{kl}(\mathbf{r})$ where C_{ijkl} is the elastic modulus tensor. Given any two deformations $u_{ij}^{(1)}$ and $u_{ij}^{(2)}$ inducing stresses $\sigma_{ij}^{(1)}$ and $\sigma_{ij}^{(2)}$, Maxwell-Betti reciprocity is the following symme-

* These authors contributed equally to this work.

† vitelli@uchicago.edu

try [24, 26, 41, 67]

$$\sigma_{ij}^{(2)}(\mathbf{r})u_{ij}^{(1)}(\mathbf{r}) = \sigma_{ij}^{(1)}(\mathbf{r})u_{ij}^{(2)}(\mathbf{r}) \quad (1)$$

To linear order, Eq. (1) is equivalent to the existence of an elastic potential energy $f(u_{ij})$ (see S.I.). When f exists, the elastic modulus tensor may be obtained as $C_{ijmn} = \frac{\partial^2 f}{\partial u_{ij} \partial u_{mn}}$, and hence it must obey the symmetry $C_{ijmn} = C_{mni j}$. However, when the microscopic interactions are active, an elastic potential energy f need not exist (see the S.I. and Ref. [66] for microscopic models). In this case, the elastic modulus tensor may be written as the sum of an even and odd contribution $C_{ijmn} = C_{ijmn}^e + C_{ijmn}^o$. The contributions that are even and odd under exchange of the first and second pairs of indices are denoted $C_{ijmn}^e = C_{mni j}^e$ and $C_{ijmn}^o = -C_{mni j}^o$, respectively. The presence of C_{ijmn}^o is known as odd elasticity [66]. Odd elasticity is the generalization of linear elasticity when Maxwell-Betti reciprocity is broken. The presence of C_{ijkl}^o implies that the solid may undergo quasistatic cycles of deformation that release energy (and absorb it if the cycle is run in reverse). The work done is proportional to the relevant entries of C_{ijmn}^o (i.e. the odd elastic moduli), as determined by the applied strain cycle [66].

Odd elastic moduli: from non-reciprocity to chirality— In 2D isotropic solids, the elastic modulus tensor can exhibit up to six independent moduli, summarized by the pictorial equation [66]:

$$\begin{pmatrix} \oplus \\ \oplus \\ \oplus \\ \oplus \end{pmatrix} = \begin{pmatrix} B & \Lambda & 0 & 0 \\ A & \Gamma & 0 & 0 \\ 0 & 0 & \mu & K^o \\ 0 & 0 & -K^o & \mu \end{pmatrix} \begin{pmatrix} \square \\ \square \\ \square \\ \square \end{pmatrix} \quad (2)$$

See the S.I. for standard tensor notation. In Eq. (2), B and μ are the familiar bulk and shear moduli. However, Eq. (2) contains four additional moduli: Λ , Γ , A , and K^o . When the system obeys Maxwell-Betti reciprocity, the matrix in Eq. (2) must be symmetrical. Hence, Maxwell-Betti reciprocity implies: $A = \Lambda$ and $K^o = 0$. Notice that Eq. (2) contains all components compatible with isotropy in two dimensions. Each of the terms capable of introducing non-reciprocity, namely A , Λ and K^o are inherently chiral. Physically, the modulus K^o corresponds to a $\pi/4$ spatial rotation between shear-stress and shear strain. Meanwhile, Λ and A connect dilation and pressure to torque and rotation.

The moduli Λ and Γ share the property that they couple to solid body rotations, represented by the second component of the strain vector in Eq. (2). Since uniform rotations do not modify the internal metric of a solid, an external field or medium, such as a substrate, is required for these moduli to be nonzero. The modulus Γ arises in couple-stress theory, a limit of Cosserat elasticity [13, 71–75]. However, A and K^o , like B and μ , can be present in a freestanding solid. Finally, notice that Γ and A both contribute to the antisymmetric stress $\epsilon_{ij}\sigma_{ij}$. For

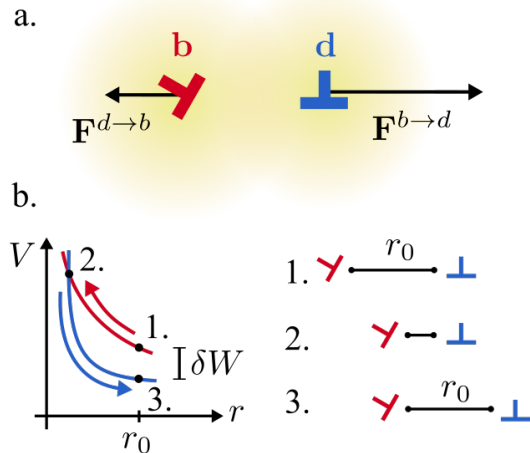


FIG. 2. **Non-reciprocal interaction between edge dislocations.** **a** Two edge dislocations in a medium with $A \neq 0$ exert Peach-Koehler forces that are not equal and opposite. As a result, when the two dislocations are moved at fixed distance, energy is extracted despite translational symmetry. **b**. Each defect sees a different potential energy $V(r)$, indicated by the color. If the translation is decomposed into two steps in which only one defect moves, the energy extracted is the difference between these potentials.

such terms to be present, the medium must be in contact with an angular momentum sink, such as internal spinning parts or a substrate. In the main text, we will set $\Gamma = \Lambda = 0$ and provide the full treatment with $\Gamma, \Lambda \neq 0$ in the S.I.

Strain distributions around defects— A topological defect is an imperfection in the underlying crystal lattice which forces the displacement field to become multivalued. A disclination is defined by an integer s such that

$$\frac{1}{2} \oint_{\Gamma} \partial_i \partial_j \epsilon_{jk} u_k dr_i = \frac{s\pi}{3} \quad (3)$$

and a dislocation is defined by a Burgers vector b_i such that

$$\oint_{\Gamma} \partial_i u_j dr_i = b_j \quad (4)$$

where Γ is a counterclockwise contour enclosing the defect. As described in the S.I., the force-balanced condition $\partial_i \sigma_{ij}(\mathbf{r}) = 0$ together with Eqs. (3-4) yield harmonic equations for displacement field for which we obtain explicit solutions. For the disclination, we find:

$$\mathbf{u}_{\text{disc}} = \frac{s}{6} r \left[\phi \hat{\phi} + \frac{1-\nu}{2} \log(r) \hat{\mathbf{r}} - \nu^o \log(r) \hat{\phi} \right] \quad (5)$$

and for the dislocation, we find

$$\mathbf{u}_{\text{disl}} = \frac{1}{2\pi} \left\{ \phi \mathbf{b} + \frac{1-\nu}{2} \log(r) \mathbf{b}^{\perp} - \frac{1+\nu}{2} (\hat{\mathbf{r}} \cdot \mathbf{b}) \hat{\phi} - \nu^o \left[\log(r) \mathbf{b} + (\hat{\phi} \cdot \mathbf{b}) \hat{\phi} \right] \right\} \quad (6)$$

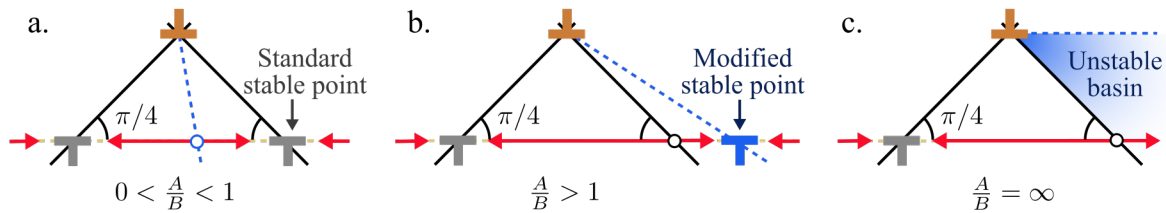


FIG. 3. **Non-reciprocity induced instability between interacting dislocations.** An orange dislocation is held stationary while a second anti-aligned dislocation is free to move along its glide plane subject to the Peach-Koehler force (red arrows). **a.** When $|A/B| < 1$, the free dislocation has two possible stable points located along rays forming an angle $\pi/4$ with the glide plane. The open circle denotes an unstable equilibrium position. The blue line forms an angle $\arctan(A/B)$ with the vertical. **b.** When $A/B > 1$, the rightmost stable equilibrium moves outward beyond $\pi/4$. **c.** When $A/B = \infty$, only one stable equilibrium position exists and the shaded region is an unstable basin.

where r and ϕ are polar coordinates about the defect and $(b_x^\perp, b_y^\perp) = (b_y, -b_x)$. In Eqs. (5-6), the elastic properties of the material enter through only two dimensionless parameters. The first is the familiar Poisson's ratio, ν , whose value is renormalized by A and K^o , see S.I. The second coefficient is a purely non-reciprocal *odd ratio* [66]

$$\nu^o = \frac{BK^o - A\mu}{\mu(B + \mu) + K^o(A + K^o)} \quad (7)$$

The terms proportional to ν in Eqs. (5-6) are inherited from reciprocal elasticity. By contrast, the last terms in Eq. (5-6) proportional to ν^o are only nonvanishing when these odd moduli are present. Qualitatively, ν^o serves as proxy for the chiral response of the material. When an odd elastic material is subject to a uniaxial compression, $\nu^o > 0$ ($\nu^o < 0$) implies the material will deflect in a clockwise (counterclockwise) manner [66].

The modification to the displacement field around a dislocation is illustrated in Fig. 1a. By taking the divergence of Eqs. (5-6) one finds that the terms proportional to ν^o vanish and so the local dilation is only affected by odd elasticity via a renormalization of ν . By contrast, odd elasticity introduces a qualitative change to the shear strain. As shown in Fig. 1b-c, we may parameterize the shear strain by an angle α that defines the local axis of elongation. We find that the moduli A and K^o rotate this axis of elongation uniformly in space. For the disclination we have:

$$\alpha_{\text{disc}} = \phi + \frac{\pi}{4}[1 + \text{sgn}(s)] + \delta\alpha \quad (8)$$

For the dislocation with \mathbf{b} parallel to $\hat{\mathbf{x}}$ axis we have

$$\alpha_{\text{disl}} = \text{sgn}(\cos \phi)\phi - \frac{\pi}{4} + \delta\alpha \quad (9)$$

In both cases, the non-reciprocal term $\delta\alpha$ is given by

$$\delta\alpha = -\frac{1}{2} \arctan\left(\frac{2\nu^o}{1 + \nu}\right) \quad (10)$$

Heuristically, this result can be rationalized by noticing that the constitutive relations in Eq. (2) entail a rotation

between shear stress and shear strain if K^o is non zero. Figure 1b-c and Fig. S2 provide numerical validation of our continuum formula for the dislocation strain field in Eq. (6). As described in the S.I., we utilize a microscopic model based on generalized Hookean springs that exert torques when elongated or compressed. Fig. 1b shows the angle α measured around two antiparallel dislocations in a honeycomb lattice of active springs. We find that angle α is shifted vertically by an amount $\delta\alpha$ when A and K^o are introduced. We note that the discontinuities in α occur when the magnitude of the shear strain vanishes, see the S.I. for an analytical expression. Figure S2 shows additional numerical measurements of the displacement gradient field in agreement with our analytical theory.

Strikingly, the effects of non-reciprocity on the strain field vanish when $\nu^o = 0$, or equivalently $A/K^o = B/\mu$. This condition applies whenever the elastic modulus tensor obeys the so-called Cauchy relations $C_{ijmn} = C_{mjin}$. These relations apply, for example, in mechanical lattices that contain only one particle per unit cell [76]. Nonetheless, as we shall see below, even when $A/K^o = B/\mu$ is satisfied, odd elasticity modifies the stress field and defect interactions.

Stress distribution around defects— We now turn to the role of non-reciprocity on the stress induced by defects. When $A = 0$, the stress tensor is symmetric and we may introduce an Airy stress function χ such that $\sigma_{ij} = \epsilon_{ik}\partial_k\epsilon_{jl}\partial_l\chi$ [17]. In the presence of disclinations and dislocations, χ obeys the equation $\Delta^2\chi(\mathbf{r}) = E s(\mathbf{r})$ where $s(\mathbf{r})$ is the defect density and E the Young's modulus renormalized by K^o , see S.I. Hence, when $A = 0$, the stress distribution in the presence of odd elasticity is indistinguishable from the reciprocal case (unless strain boundary conditions are imposed on the medium).

However, when $A \neq 0$ is nonzero, the stress distribution receives a nontrivial modification. Utilizing the strain field, we may compute the stress directly via the constitutive relations $\sigma_{ij} = C_{ijkl}u_{kl}$, see S.I. The effect of A is twofold. First, the local pressure is unchanged and the local axis of shear-stress is rotated by an angle $\arctan(A/B)/2$. Second, the modulus A introduces a torque density $\tau = \epsilon_{ij}\sigma_{ij}$ that for the disclination

reads $\tau_{\text{disc}}(\mathbf{r}) = A(1 - \nu)(2s/3)\log(r)$ and for the dislocation reads $\tau_{\text{disl}}(\mathbf{r}) = A(1 - \nu)\hat{\phi} \cdot \mathbf{b}/\pi r$. In both cases, $\frac{\tau(\mathbf{r})}{P(\mathbf{r})} = \frac{2A}{B}$, where P is the pressure.

Extracting work from non-reciprocal defect interactions—In standard elasticity, one can compute the forces between two defects by taking gradients of their interaction energy. Yet, in the presence of odd elasticity, the interaction energy cannot be defined. Nonetheless, we can compute the forces directly via the stress distribution. First consider an isolated dislocation exposed to an external stress field $\sigma_{mk}^{(\text{ext})}$ in mechanical equilibrium $\partial_m \sigma_{mk}^{(\text{ext})} = 0$. The work done by the material in moving the dislocation by $\delta \mathbf{x}$ is given by $\delta W = \mathbf{f} \cdot \delta \mathbf{x}$, where \mathbf{f} is the so-called Peach-Koehler force $f_m = \epsilon_{mi} \sigma_{ij}^{(\text{ext})} b_j$ [2, 17, 77]. From the force balance equation $\partial_i \sigma_{ij} = 0$, we find that the Peach-Koehler force is curl free $\nabla \times \mathbf{f} = 0$. Since \mathbf{f} is curl free, the force on a single dislocation may be derived from a potential regardless of the nature of the elasticity, see S.I. Notice furthermore that the Peach-Koehler force is agnostic to the elasticity of the medium and rely solely on the principle of virtual work and on the defining property of the dislocation in Eq. (4) [2, 17].

Now, suppose we have dislocations with Burgers vectors \mathbf{b}_1 and \mathbf{b}_2 with relative coordinate \mathbf{r} pointing from the former to the latter. To obtain the force on one dislocation, we simply evaluate the Peach-Koehler with the stress produced by the other. For systems with Maxwell-Betti reciprocity, the total interaction energy may be written as a potential $V(\mathbf{r})$ that depends only the separation between the two dislocations. Consequently, the Peach-Koehler forces on each of the two dislocations are equal and opposite, i.e. $\mathbf{f}^{b_1 \rightarrow b_2} = -\mathbf{f}^{b_2 \rightarrow b_1}$. However, when $A \neq 0$, we find that $\mathbf{f}^{b_1 \rightarrow b_2} \neq -\mathbf{f}^{b_2 \rightarrow b_1}$ and that there is a net force on the pair of dislocations:

$$\mathbf{f}^{b_1 \rightarrow b_2} + \mathbf{f}^{b_2 \rightarrow b_1} = (1 - \nu)A\hat{\mathbf{r}} \frac{\mathbf{b}_2 \times \mathbf{b}_1}{\pi r} \quad (11)$$

As depicted in Fig. 2, Eq. (11) implies that manually sliding the two dislocations in the same direction while maintaining their relative separation will either do work on or extract energy from the active medium given by

$$\delta W = (1 - \nu)A(\delta \mathbf{x} \cdot \hat{\mathbf{r}}) \frac{\mathbf{b}_2 \times \mathbf{b}_1}{\pi r} \quad (12)$$

where $\delta \mathbf{x}$ is the motion of the center of the defects.

At first sight, Eq. (11) appears somewhat paradoxical. Since $\nabla \times \mathbf{f} = 0$, the force on either dislocation may be derived from gradients of a potential that depends only on their relative separation. So how can energy be extracted while maintaining their separations? The crucial point is the following: while the individual forces on a given dislocation may be expressed as a gradient of a potential, the potentials that each dislocation experiences are *different* (see Fig. 2b). Furthermore, we note that Eq. (11) resembles a violation of Newton's third law. This is possible since dislocations do not carry mass, so their motion does not entail sources of linear momentum, which do not arise

from odd elasticity. The full modification of the defect interaction with $A \neq 0$ derived in the S.I. is

$$\mathbf{f}^{a, b_1 \rightarrow b_2} = \frac{(1 - \nu)A}{2\pi r} \left\{ (\mathbf{b}_2 \times \mathbf{b}_1) \hat{\mathbf{r}} + [(\mathbf{b}_1 \cdot \mathbf{b}_2) - 2(\mathbf{b}_1 \cdot \hat{\mathbf{r}})(\mathbf{b}_2 \cdot \hat{\mathbf{r}})] \hat{\phi} \right\} \quad (13)$$

Mechanical (in)stability of dislocation-pairs—Even for parallel dislocations, $\mathbf{b}_2 \times \mathbf{b}_1 = 0$, the effects of A are still apparent. As an illustration, in Fig. 3 we examine the effect of non-reciprocity on two dislocations with parallel glide planes. When $A = 0$, the dislocations obey the classic result: their separation vector forms an angle $\pi/4$ with respect to their glide planes [2, 17]. When $0 < A/B < 1$, the mechanically stable positions remain the same while their basins of attraction change. When $A/B > 1$, the right equilibrium point moves out beyond the $\pi/4$ angle. When $A/B \rightarrow \infty$, the rightmost basin becomes altogether unstable. We note that the non-reciprocity in Eq. (11) is present already in the continuum theory without any reference to microscopics. Since defect motion involves rearrangements of bonds at a microscopic scale, we assume that the defect motion shown in Fig. 3 occurs along the glide plane of the defect, onto which the Peach-Koehler force is projected.

Point defects: local dilations and torques—Unlike topological defects, local perturbations such as torques or dilations do not require a multivalued displacement field, yet still exhibit long-range effects agnostic to microscopic details. Local dilations can arise, for example, from (non-topological) point defects such as inclusions, interstitials, or vacancies. Moreover, in systems violating angular momentum conservation, such as those exhibiting A or Γ , defect cores can exhibit local torques not captured by the continuum torque density $\tau(\mathbf{r}) = \epsilon_{ij} \sigma_{ij}(\mathbf{r})$. In the S.I., we show that the torque and area change of a defect core are coupled in nonreciprocal isotropic media through the relation:

$$\tau^c = \mu\varphi + K^o\Omega \quad (14)$$

In Eq. (14), τ^c is the torque exerted by the core, while $\nabla \cdot \mathbf{u} = \Omega\delta(\mathbf{r})$ and $\nabla \times \mathbf{u} = \varphi\delta(\mathbf{r})$ are, respectively, the dilation and rotation experienced by the core. Notice that when $\mu = 0$, a torque at the core necessarily implies core dilation. For our microscopic construction of the dislocation analyzed in Fig. 1 and Fig. S2 we empirically find that $\tau^c = 0$. However, in general, one cannot exclude a nonzero torque at the core of disclinations and dislocations when sources of angular momentum are present. Note that Ω and φ modify the stress and strain fields of defects and their interactions (see S.I.). For example, the displacement field of a (non-topological) point defect associated with microscopic dilations and torques reads

$$\mathbf{u}_{\text{point}}(\mathbf{r}) = \frac{\Omega\hat{\mathbf{r}} + \varphi\hat{\phi}}{2\pi r} \quad (15)$$

Comparison to vortex lattices and gyroelastic media — Odd elasticity is a modification to the relationship between stress and strain in an elastic solid. This modification is inherently non-conservative and therefore cannot be captured by standard Lagrangian or Hamiltonian techniques. By contrast, consider the following simplified Lagrangian, which captures the transverse interactions characteristic of vortex lattices [78–100] or gyroelastic media [101–109]:

$$\mathcal{L} = -\frac{1}{2}\epsilon_{ij}u_i\partial_t u_j - \frac{1}{2}C_{ijkl}^e\partial_i u_j\partial_k u_l \quad (16)$$

where $C_{ijkl}^e = C_{klij}^e$. The *inertial* equation of motion corresponding to Eq. (16) is given by $\epsilon_{jm}\partial_t u_m = \partial_i C_{ijkl}^e\partial_k u_l$, which states that the motion is transverse to the conservative elastic force. Note that this equation of motion may be rewritten in the form $\partial_t u_j = \partial_i \tilde{C}_{ijkl}\partial_k u_l$ where $\tilde{C}_{ijkl} = \epsilon_{mj}C_{imkl}^e$. If C_{ijkl}^e describes standard isotropic elasticity with only the bulk B and shear μ moduli, then the effective elastic modulus tensor \tilde{C}_{ijkl} contains entries that formally resemble the odd moduli $\tilde{A} = B$ and $\tilde{K}^o = \mu$. While the equations of motion of a conservative system with transverse interactions seems at first sight equivalent to an *overdamped* solid with odd elasticity, the stress-strain relations of the two systems are manifestly different. In particular, we highlight the following crucial physical distinction. If one defines an effective stress $\tilde{\sigma}_{ij} = \tilde{C}_{ijkl}u_{kl}$ and computes (for an Hamiltonian system with transverse interactions) the quantity $\delta\tilde{w} = -\tilde{\sigma}_{ij}\delta u_{ij}$, the result does not correspond to physical energy as it would in odd elasticity. The displacement fields around defects we calculated in Eqs. (5-6,15) for odd elastic solids still apply to the conservative systems governed by Eq. (16). However, since $\tilde{\nu}^o = 0$, there are no modifications of the static elastic distortions. Likewise, while the effective forces in Eqs. (11-13) are still present because they depend on $\tilde{A} = B$, the energy-extraction formula Eq. (12) no longer holds.

Conclusion — To summarize, we showed how violations of Maxwell-Betti reciprocity affect the mechanics and stability of crystalline defects, paving the way for active generalizations of plasticity and defect-mediated melting.

Acknowledgments — V.V. acknowledges support from the Simons Foundation, the Complex Dynamics and Systems Program of the Army Research Office under grant W911NF-19-1-0268, and the University of Chicago Materials Research Science and Engineering Center, which is funded by the National Science Foundation under Award No. DMR-2011854. C.S. was supported by the National Science Foundation Graduate Research Fellowship under Grant No. 1746045. L.B. acknowledges support from the Heising-Simons Scholarship and the James Franck Institute Undergraduate Summer Research Award. The authors would like to thank B. Vansaders, M. Han and M. Fruchart for helpful conversations.

Supplementary Information

S1. NONRECIPROCAL ELASTICITY

The starting place of our work is linear Cauchy elasticity. Throughout, we use $u_i(\mathbf{r})$ to denote the displacement field, which describes the deformation of a solid. Our work is predicated on two assumptions: (i) linear momentum is conserved in the medium, and therefore the elastic force density may be written as $f_j(\mathbf{r}) = \partial_i \sigma_{ij}(\mathbf{r})$ for a stress $\sigma_{ij}(\mathbf{r})$; and (ii) no stresses are induced by solid-body translations. Using assumption (ii), we may expand $\sigma_{ij}(\mathbf{r})$ to lowest order in gradients of the displacement field $u_i(\mathbf{r})$ to obtain:

$$\sigma_{ij}(\mathbf{r}) = C_{ijmn} u_{mn}(\mathbf{r}) \quad (\text{S1})$$

where $u_{mn} = \partial_m u_n$ and C_{ijmn} is the phenomenological coefficient known as the elastic modulus tensor. As discussed in the main text, we decompose the elastic modulus tensor as $C_{ijmn} = C_{ijmn}^e + C_{ijmn}^o$ where $C_{ijmn}^e = C_{mni j}^e$ while $C_{ijmn}^o = -C_{mni j}^o$. To motivate this decomposition, we consider the work associated with deformation δu_{ij} of an area \mathcal{V} , given by

$$\delta W = \int_{\mathcal{V}} f_i \delta u_i dA \quad (\text{S2})$$

$$= \int_{\partial \mathcal{V}} \hat{n}_i \sigma_{ij} \delta u_j dl - \int_{\mathcal{V}} \sigma_{ij} \delta u_{ij} dA \quad (\text{S3})$$

where \hat{n}_i is the outward normal. Equation (S3) shows that the work done per unit area by the elastic forces in the bulk of the material is given by $\delta w = -\sigma_{ij} \delta u_{ij}$ [110]. If a unit of material is brought through a quasistatic cycle of strain $u_{ij}(t)$ such that $u_{ij}(0) = u_{ij}(T_f)$, then the total work done is:

$$w = \int_0^{T_f} \frac{dw}{dt} dt \quad (\text{S4})$$

$$= -C_{ijkl} \int_0^{T_f} u_{kl} \frac{du_{ij}}{dt} dt \quad (\text{S5})$$

$$= -\frac{C_{ijkl}^e}{2} [u_{ij} u_{kl}]_0^{T_f} - \frac{C_{ijkl}^o}{2} \int_0^{T_f} u_{kl} \frac{du_{ij}}{dt} dt \quad (\text{S6})$$

$$= -\frac{C_{ijkl}^o}{2} \int_0^{T_f} u_{kl} \frac{du_{ij}}{dt} dt \quad (\text{S7})$$

where we have used the fact that $u_{ij}(0) = u_{ij}(T_f)$. Hence, when $C_{ijkl}^o = 0$, the work done vanishes on every closed cycle, and therefore an elastic potential may be defined. When C_{ijkl}^o is nonzero, a cycle may be found on which net work is done by the material [66]. Hence, the constitutive relation $\sigma_{ij} = C_{ijkl} u_{kl}$ follows from an energy if and only if $C_{ijkl}^o = 0$.

A. Isotropic 2D elastic modulus tensor

Here we discuss the form of the elastic modulus tensor C_{ijmn} in two-dimensional isotropic materials. In following Eq. (2) of the main text, we will use the following basis for two-by-two matrices:

$$\tau_{ij}^0 = \begin{pmatrix} 1 & 0 \\ 0 & 1 \end{pmatrix}, \quad \tau_{ij}^1 = \begin{pmatrix} 0 & -1 \\ 1 & 0 \end{pmatrix}, \quad \tau^2 = \begin{pmatrix} 1 & 0 \\ 0 & -1 \end{pmatrix}, \quad \tau_{ij}^3 = \begin{pmatrix} 0 & 1 \\ 1 & 0 \end{pmatrix} \quad (\text{S8})$$

Using the τ_{ij}^α , we define $u^\alpha = \tau_{ij}^\alpha u_{ij}$ and $\sigma^\alpha = \tau_{ij}^\alpha \sigma_{ij}$. In this basis, the elastic modulus tensor may be expressed as a four-by-four matrix $C^{\alpha\beta} = \frac{1}{2} \tau_{ij}^\alpha C_{ijmn} \tau_{mn}^\beta$. Thus, the constitutive equations may be written as:

$$\begin{pmatrix} \sigma^0 \\ \sigma^1 \\ \sigma^2 \\ \sigma^3 \end{pmatrix} = \begin{pmatrix} C^{00} & C^{01} & C^{02} & C^{03} \\ C^{10} & C^{11} & C^{12} & C^{13} \\ C^{20} & C^{21} & C^{22} & C^{23} \\ C^{30} & C^{31} & C^{32} & C^{33} \end{pmatrix} \begin{pmatrix} u^0 \\ u^1 \\ u^2 \\ u^3 \end{pmatrix}. \quad (\text{S9})$$

The pictorial notation in the main text corresponds to the physical interpretation of each component: u^0 (□) represents dilation, u^1 (◻) represents rotation, and u^2 (▭) represents shear strain with an axis of elongation in the x -direction, and u^3 (▭) represents shear strain with an axis of elongation at a positive 45° angle. Similarly, σ^0 (⊕) represents the isotropic stress (negative of pressure), σ^1 (⊗) represents an internal torque density, and σ^2 (⊕) and σ^3 (⊗) represent shear stresses.

Notice that $C^{\alpha\beta}$ has 16 independent components when no physical restrictions are imposed. The condition for Maxwell-Betti reciprocity, i.e. $C_{ijmn} = C_{mnij}$ is equivalent to $C^{\alpha\beta} = C^{\beta\alpha}$. Hence, when Maxwell-Betti reciprocity holds, $C^{\alpha\beta}$ has only 10 independent components. If the stress is required to be symmetric, then $C^{1\alpha} = 0$ for all α and if there is no coupling to rotation, then $C^{\alpha 1} = 0$ for all α .

Next, we consider the role of isotropy, which states that the elastic modulus tensor is invariant under rotations. Upon a passive rotation of the coordinate system through angle θ , the elastic modulus tensor transforms as

$$C'_{ijmn} = R_{ik}R_{jl}R_{mp}R_{nq}C_{klpq} \text{ where } R_{ij} = \begin{pmatrix} \cos \theta & \sin \theta \\ -\sin \theta & \cos \theta \end{pmatrix}. \quad (\text{S10})$$

Hence $C^{\alpha\beta}$ transforms as $C'^{\alpha\beta} = R^{\alpha\gamma}R^{\beta\sigma}C^{\gamma\sigma}$, where

$$R^{\alpha\beta} = \begin{pmatrix} 1 & 0 & 0 & 0 \\ 0 & 1 & 0 & 0 \\ 0 & 0 & \cos 2\theta & \sin 2\theta \\ 0 & 0 & -\sin 2\theta & \cos 2\theta \end{pmatrix}. \quad (\text{S11})$$

Requiring that $C'^{\alpha\beta} = C^{\alpha\beta}$ for all θ implies that $C^{\alpha\beta}$ must take the form:

$$C^{\alpha\beta} = 2 \begin{pmatrix} B & \Lambda & 0 & 0 \\ A & \Gamma & 0 & 0 \\ 0 & 0 & \mu & K^o \\ 0 & 0 & -K^o & \mu \end{pmatrix}. \quad (\text{S12})$$

Finally, we note that $C_{ijmn} = \frac{1}{2}\tau_{ij}^\alpha\tau_{mn}^\beta C^{\alpha\beta}$. Thus, in standard tensor notation, the elastic modulus tensor reads:

$$C_{ijmn} = B\delta_{ij}\delta_{mn} + \mu(\delta_{im}\delta_{jn} + \delta_{jm}\delta_{in} - \delta_{ij}\delta_{mn}) - A\epsilon_{ij}\delta_{mn} + K^o E_{ijmn} + \Gamma\epsilon_{ij}\epsilon_{mn} - \Lambda\delta_{ij}\epsilon_{mn} \quad (\text{S13})$$

where

$$E_{ijmn} = \frac{1}{2}(\epsilon_{im}\delta_{jn} + \epsilon_{in}\delta_{jm} + \epsilon_{jm}\delta_{in} + \epsilon_{jn}\delta_{im}). \quad (\text{S14})$$

Finally, we discuss an additional symmetry known as the Cauchy relations, defined by $C_{ijmn} = C_{mjin}$. The Cauchy relations arise, for example, in situations in which every particle in a lattice is an inversion center, see, e.g., Sec III of Ref. [76]. Setting $C_{ijmn} - C_{mjin} = 0$, we find that the Cauchy relations in isotropic media imply:

$$0 = B + \Gamma - 2\mu \quad (\text{S15})$$

$$0 = A - 2K^o - \Lambda \quad (\text{S16})$$

To see in brief the origin of the Cauchy relations for the case of a monatomic crystal, note that the force-displacement relationship may be expressed via a dynamical matrix $F_i(\mathbf{r}) = \sum_{\mathbf{r}'} D_{ij}(\mathbf{r} - \mathbf{r}')u_j(\mathbf{r}')$. Then at low wave numbers in Fourier space, we have

$$F_i(\mathbf{q}) = q_k \left[\frac{\partial^2 D_{ij}}{\partial q_k \partial q_l} \right]_{\mathbf{q}=0} q_l u_j(\mathbf{q}). \quad (\text{S17})$$

Identifying $F_i(\mathbf{q}) = q_k \sigma_{kj}(\mathbf{q})$ and $u_j(\mathbf{q}) = q_l u_j(\mathbf{q})$, we find that $C_{ijkl} = \left[\frac{\partial^2 D_{jl}}{\partial q_i \partial q_k} \right]_{\mathbf{q}=0}$, which is manifestly symmetric under the exchange of the first and third indices.

2. DEFECTS IN ISOTROPIC 2D NONRECIPROCAL CRYSTALS

A. Mechanical stability

A topological defect is a local imperfection in a crystal that has an effect on the stress and strain at large length scales. Near the local imperfection, there is a region of high deformation, known as the core, whose description lies

beyond the continuum theory. Nonetheless, we may work in the limit that the core size is arbitrarily small compared to the distances of interest. In this limit, we may approximate the stresses in the medium as $\sigma_{ij}(\mathbf{r}) = C_{ijkl}\partial_k u_l(\mathbf{r})$ for all $\mathbf{r} \neq \mathbf{r}^c$, where \mathbf{r}^c is the location of the defect. By contrast, the macroscopic constitutive relations are assumed not to apply at the defect core itself $\mathbf{r} = \mathbf{r}^c$. To derive the displacement, strain, and stress field about a defect, a notion of mechanical equilibrium is required. For our purposes, a medium is in mechanical equilibrium when the net force and torque on every subset of the medium vanishes. As described in Section S1, we assume that the elastic medium conserves linear momentum, and hence the net force on any patch of material \mathcal{V} is given by the flux of the stress through its boundary:

$$F_j = \oint_{\partial\mathcal{V}} \hat{n}_i \sigma_{ij} d\ell \quad (\text{S18})$$

where \hat{n}_i is the outward normal. However, we will generically not assume that angular momentum is conserved. In this case, the net torque on \mathcal{V} is the sum of two contributions: the flux of angular momentum at its boundary and the sources integrated over its area:

$$T = - \oint_{\partial\mathcal{V}} \hat{n}_i \sigma_{ij} \epsilon_{jk} r_k d\ell - \int_{\mathcal{V}} \tau(\mathbf{r}) dA \quad (\text{S19})$$

The first term of Eq. (S19) is the angular momentum drawn from neighboring patches of material, while $\tau(\mathbf{r})$ is the angular momentum drawn from external sources (such as a substrate or internal spinning parts). For $\mathbf{r} \neq 0$ (i.e. outside the core), we have $\tau(\mathbf{r}) = \epsilon_{ij} \sigma_{ij}(\mathbf{r})$. Hence, if \mathcal{V} does not contain the topological defect, then we may apply Stokes' theorem to Eq. (S18) and Eq. (S19) to obtain:

$$F_j = \int_{\mathcal{V}} \partial_i \sigma_{ij} dA \quad (\text{S20})$$

and

$$T = - \int_{\mathcal{V}} (\partial_i \sigma_{ij}) \epsilon_{jk} r_k dA \quad (\text{S21})$$

Since Eqs. (S20-S21) apply for all choices of \mathcal{V} that do not enclose the defect core, we find that a necessary condition for mechanical equilibrium is:

$$\partial_i \sigma_{ij}(\mathbf{r}) = 0 \text{ for all } \mathbf{r} \neq 0. \quad (\text{S22})$$

However, note that Eq. (S22) is necessary but not sufficient to ensure mechanical stability. When \mathcal{V} encloses the topological defect, we must directly apply Eq. (S18) and Eq. (S19). In this case, Eq. (S19) takes the form:

$$T = - \oint_{\partial\mathcal{V}} \hat{n}_i \sigma_{ij} \epsilon_{jk} r_k d\ell - \int_{\mathcal{V} \setminus \mathbf{r}^c} \epsilon_{ij} \sigma_{ij} dA - \tau^c \quad (\text{S23})$$

where \mathbf{r}^c is the defect location and τ^c is the net torque associated with the core of the defect.

In Sections S2 B-S2 E below we explicitly solve for the displacement, strain, and stress field for disclinations, dislocation, local dilations (e.g. interstitials) and torques. In Sections S2 B-S2 C we solve for dislocations and disclinations while setting $\Lambda = \Gamma = 0$ and $\tau^c = 0$. In Section S2 D, we then consider the modifications introduced by nonzero Λ and Γ . Finally, in Section S2 E, we provide solutions for local dilations and rotations and discuss how nonzero τ^c affects the solutions for the dislocations and disclinations.

B. Disclination

We first consider the stress and strain field about a disclination centered at the origin. Assuming an underlying crystal with C_6 symmetry, a disclination is described by an integer s such that

$$\frac{s\pi}{3} = \frac{1}{2} \oint_{\gamma} \epsilon_{ij} \partial_k \partial_i u_j dr_k \quad (\text{S24})$$

where γ is an arbitrary counterclockwise path enclosing the disclination at the origin [1]. Equation (S24) implies that the disclination takes the form

$$u_i(\mathbf{r}) = -\frac{s}{6} \phi \epsilon_{ik} r_k + v_i(\mathbf{r}), \quad (\text{S25})$$

where ϕ is the polar angle and $v_i(\mathbf{r})$ is a single-valued function. The constitutive relation $\sigma_{ij}(\mathbf{r}) = C_{ijkl}\partial_k u_l(\mathbf{r})$ together with the force balance equation $\partial_i \sigma_{ij}(\mathbf{r}) = 0$ yields the following differential equation for $v_i(\mathbf{r})$:

$$\Delta(\partial_i v_i) = \frac{s}{3} \left(\frac{1-\nu}{2} \right) \delta(\mathbf{r}) \quad (\text{S26})$$

$$\Delta(\partial_i \epsilon_{ij} v_j) = -\frac{s}{3} \nu^\circ \delta(\mathbf{r}) \quad (\text{S27})$$

where ν and ν° are, respectively, the Poisson's and odd ratios given by:

$$\nu \equiv \frac{\mu(B-\mu) + K^\circ(A-K^\circ)}{\mu(B+\mu) + K^\circ(A+K^\circ)} \quad (\text{S28})$$

$$\nu^\circ \equiv \frac{BK^\circ - A\mu}{\mu(B+\mu) + K^\circ(A+K^\circ)} \quad (\text{S29})$$

Requiring that $\hat{n}_i \sigma_{ij}$ vanishes along a circle of radius R , we obtain the following solution:

$$u_i(\mathbf{r}) = \frac{s}{6} \left\{ -\phi \epsilon_{ij} x_j + \frac{(1-\nu)}{2} r_i \log(r/R_1) + \nu^\circ \epsilon_{ij} r_j \log(r/R_2) \right\} \quad (\text{S30})$$

Here, $R_1 = R_2 = R/\sqrt{e}$ are constants introduced to ensure the stress boundary conditions are satisfied. However, as discussed in Section S2 E, R_1 and R_2 receive corrections in the presence of nonzero τ^c . Using $\sigma_{ij} = C_{ijmn}\partial_m u_n$, we obtain the stress:

$$\sigma_{ij}(\mathbf{r}) = (1-\nu) \frac{s}{12} \left\{ B \left[2 \log(r/R_1) \delta_{ij} - \left(\frac{2r_i r_j}{r^2} - \delta_{ij} \right) \right] - A \left[2 \log(r/R_2) \epsilon_{ij} + \frac{r_i \epsilon_{jll} r_l + r_j \epsilon_{ill} r_l}{r^2} \right] \right\} \quad (\text{S31})$$

The effects of K° and A on the stress and strain have geometric interpretations. First, we note that K° and A only modify the pressure $P(\mathbf{r}) = -\sigma_{ii}(\mathbf{r})/2 = -(1-\nu)sB \log(r)/12$ through the coefficient ν and leave the functional form of $P(\mathbf{r})$ unchanged. Furthermore, the ratio of the isotropic stress to the internal torque density $\tau(\mathbf{r}) = \epsilon_{ij}\sigma_{ij}(\mathbf{r})$ is constant in space and is given by the ratio:

$$\frac{\tau(\mathbf{r})}{P(\mathbf{r})} = \frac{2A}{B} \quad (\text{S32})$$

Moreover, let us define the quantities $S_{ij}^r = \frac{2r_i r_j}{r^2} - \delta_{ij}$ and $S_{ij}^\phi = (\epsilon_{ik} r_k r_j + \epsilon_{jk} r_k r_i)/r^2$. The tensors S_{ij}^r and S_{ij}^ϕ form a basis for local shears (i.e. traceless symmetric tensors) with S_{ij}^r containing an axis of extension in the direction \hat{r}_i and S_{ij}^ϕ containing an axis of extension along $(\hat{r}_i - \hat{\phi}_i)/\sqrt{2}$. When $A = 0$, Eq. (S31) shows that the shear stress is entirely proportional to S_{ij}^r . However, when A is nonzero, the axis of shear is everywhere rotated through an angle $\delta\theta$ given by:

$$\delta\theta(\mathbf{r}) = -\frac{1}{2} \arctan \left(\frac{S_{ij}^\phi(\mathbf{r})\sigma_{ij}(\mathbf{r})}{S_{ij}^r(\mathbf{r})\sigma_{ij}(\mathbf{r})} \right) = -\frac{1}{2} \arctan \left(\frac{A}{B} \right) \quad (\text{S33})$$

We can apply a similar analysis to the displacement gradient $\partial_i u_j(\mathbf{r})$. Like the pressure, K° and A only modify the dilation $\partial_i u_i(\mathbf{r}) = (1-\nu)s \log(r)/3$ through the constant ν . Furthermore, A and K° induce a local rotation of the axis of shear strain given by:

$$\delta\alpha(\mathbf{r}) = -\frac{1}{2} \arctan \left(\frac{S_{ij}^\phi(\mathbf{r})\partial_i u_j(\mathbf{r})}{S_{ij}^r(\mathbf{r})\partial_i u_j(\mathbf{r})} \right) = -\frac{1}{2} \arctan \left(\frac{2\nu^\circ}{1+\nu} \right) \quad (\text{S34})$$

as appears in Eq. (9) of the main text.

C. Dislocation

A dislocation is defined by a Burgers vector b_i such that:

$$\oint_\gamma \partial_i u_j dr_i = b_j \quad (\text{S35})$$

Condition Eq. (S35) implies that the solution for u_i is of the form:

$$u_i(\mathbf{r}) = \frac{b_i}{2\pi}\phi + v_i(\mathbf{r}) \quad (\text{S36})$$

where once again $v_i(\mathbf{r})$ is a single-valued function. The requirement that $\partial_i\sigma_{ij}(\mathbf{r}) = 0$ for $\mathbf{r} \neq 0$ yields the following differential equation for $v_i(\mathbf{r})$:

$$\Delta(\partial_i v_i) = \nu b_i \epsilon_{ij} \partial_j \delta(\mathbf{r}) \quad (\text{S37})$$

$$\Delta(\partial_i \epsilon_{ij} v_j) = (-b_i + 2\nu^o \epsilon_{ij} b_j) \partial_i \delta(\mathbf{r}) \quad (\text{S38})$$

Requiring that $\partial_i v_i$ and $\partial_i \epsilon_{ij} v_j$ fall off to 0 at $r \rightarrow \infty$, we obtain the resulting solution for the displacement field:

$$u_i(\mathbf{r}) = \frac{1}{2\pi} \left\{ b_i \phi + \epsilon_{ik} b_k \frac{(1-\nu)}{2} \log(r) + \frac{(1+\nu)}{2} \frac{\epsilon_{im} r_m b_n r_n}{r^2} - \nu^o \left[b_i \log(r) - \frac{\epsilon_{im} r_m r_n \epsilon_{nk} b_k}{r^2} \right] \right\} \quad (\text{S39})$$

and the stress is given by:

$$\sigma_{ij}(\mathbf{r}) = \frac{(1-\nu)}{2\pi r^2} \left\{ B \left[r_m \epsilon_{mn} b_n \delta_{ij} - b_k r_k \left(\frac{r_i \epsilon_{jm} r_m + r_j \epsilon_{im} r_m}{r^2} \right) \right] - A \left[r_m \epsilon_{mn} b_n \epsilon_{ij} - b_k r_k \left(\frac{2r_i r_j}{r^2} - \delta_{ij} \right) \right] \right\} \quad (\text{S40})$$

Here, when $A = 0$, the shear stress is entirely proportional to $S_{ij}^\phi(\mathbf{r})$. As with the disclination, when A is nonzero the ratio of the torque to the pressure is given by $\tau(\mathbf{r})/P(\mathbf{r}) = 2A/B$ and the shear stress is rotated by an angle $\delta\theta(\mathbf{r}) = -\arctan(A/B)/2$. Moreover, the local dilation is unmodified by A and K^o (except through the value of ν) and the shear strain is locally rotated by $\delta\alpha(\mathbf{r}) = -\arctan[2\nu^o/(1+\nu)]/2$.

D. Coupling to rotations

In this section, we consider the role of the moduli Λ and Γ . These moduli imply that solid-body rotations induce pressure and torque, respectively. Since solid-body rotations do not change the intrinsic geometry of a solid, such couplings require that the solid be in contact with an additional field or background medium, such as a substrate. Notice that disclinations require that the bond-angle field $\epsilon_{ij}\partial_i u_j$ become multivalued. In other words, the microscopic structure must be mechanically equivalent when rotated through an angle $s\pi/3$. Thus, a treatment of disclinations necessarily requires either no coupling to rotations or a non-monotonic stress-rotation coupling in order to ensure the equivalence of mechanical states related by finite rotations. Therefore, the linear coefficients Λ and Γ are not sufficient to study disclinations in media that couple to rotations. By contrast, the bond-angle field $\epsilon_{ij}\partial_i u_j$ remains single-valued for dislocations. Hence, dislocations can still be self-consistently treated using the linear coupling captured by Λ and Γ . Below we present the role of Λ and Γ on dislocations. Moreover, in Section S2E, we will see that the local dilations and torques are unmodified by Λ and Γ .

Using the full elastic modulus tensor in Eq. (S13), the generalization of Eqs. (S37-S38) is

$$\Delta(\partial_i v_i) = b_i (\nu \epsilon_{ij} - 2\gamma_1 \delta_{ij}) \partial_j \delta(\mathbf{r}) \quad (\text{S41})$$

$$\Delta(\partial_i \epsilon_{ij} v_j) = b_i (2\nu^o \epsilon_{ij} - \gamma_2 \delta_{ij}) \partial_j \delta(\mathbf{r}) \quad (\text{S42})$$

where we now have the quantities:

$$\nu = \frac{(B-\mu)(\mu+\Gamma) + (A-K^o)(K^o-\Lambda)}{(B+\mu)(\mu+\Gamma) + (A+K^o)(K^o-\Lambda)} \quad (\text{S43})$$

$$\nu^o = \frac{BK^o - A\mu}{(B+\mu)(\mu+\Gamma) + (A+K^o)(K^o-\Lambda)} \quad (\text{S44})$$

$$\gamma_1 = \frac{K^o\Gamma + \Lambda\mu}{(B+\mu)(\mu+\Gamma) + (A+K^o)(K^o-\Lambda)} \quad (\text{S45})$$

$$\gamma_2 = \frac{(B+\mu)(\mu-\Gamma) + (A+K^o)(K^o+\Lambda)}{(B+\mu)(\mu+\Gamma) + (A+K^o)(K^o-\Lambda)} \quad (\text{S46})$$

Notice that $\gamma_1 \rightarrow 0$ and $\gamma_2 \rightarrow 1$ when $\Lambda, \Gamma \rightarrow 0$. Solving Eqs. (S41-S42) with $\Lambda, \Gamma \neq 0$ then yields the displacement field:

$$u_i(\mathbf{r}) = \frac{1}{2\pi} \left[b_i \phi + \frac{(\gamma_2 - \nu)}{2} \epsilon_{ik} b_k \log(r) - (\nu^o + \gamma_1) b_i \log(r) + \frac{(\gamma_2 + \nu)}{2} \frac{r_k b_k \epsilon_{il} r_l}{r^2} + (\nu^o - \gamma_1) \frac{b_k r_k r_i}{r^2} \right] \quad (\text{S47})$$

The strain field is characterized by the following three quantities. The dilation is given by:

$$\partial_m u_m = \frac{1}{2\pi r^2} [(1 - \nu)r_m \epsilon_{mk} b_k - 2\gamma_1 b_m r_m] \quad (\text{S48})$$

The rotation is given by:

$$\epsilon_{mn} \partial_m u_n = \frac{-1}{2\pi r^2} [(1 + \gamma_2)r_m b_m + 2\nu^o r_m \epsilon_{mn} b_n] \quad (\text{S49})$$

The shear strain is given by:

$$\frac{\partial_m u_n + \partial_n u_m - \delta_{mn} \partial_i u_i}{2} = -\frac{1}{4\pi r^2} \left\{ [2\nu^o b_k r_k + (\gamma_2 - 1)b_j \epsilon_{jk} r_k] \left(\frac{2r_m r_n}{r^2} - \delta_{mn} \right) + [(1 + \nu)b_k r_k + 2\gamma_1 b_j \epsilon_{jk} r_k] \left(\frac{r_m \epsilon_{nk} r_k + r_n \epsilon_{mk} r_k}{r^2} \right) \right\} \quad (\text{S50})$$

The stress is characterized by the following three quantities. The isotropic stress:

$$\sigma_{ii} = \frac{1}{\pi r^2} \{ [B(1 - \nu) + 2\Lambda\nu^o] r_m \epsilon_{mn} b_n - [2B\gamma_1 - \Lambda(1 + \gamma_2)] r_m b_m \} \quad (\text{S51})$$

The torque density:

$$\epsilon_{ij} \sigma_{ij} = \frac{1}{\pi r^2} \{ -[A(1 - \nu) + 2\Gamma\nu^o] r_m \epsilon_{mn} b_n + [2A\gamma_1 - \Gamma(1 + \gamma_2)] r_m b_n \} \quad (\text{S52})$$

And the shear stress:

$$\frac{\sigma_{ij} + \sigma_{ji} - \delta_{ij} \sigma_{mm}}{2} = -\frac{1}{2\pi r^2} \left\{ [(2\Gamma\nu^o - A(1 - \nu))b_k r_k + (\Gamma(1 + \gamma_2) + 2A\gamma_1)b_j \epsilon_{jk} r_k] \left(\frac{2r_i r_j}{r^2} - \delta_{ij} \right) + [(B(1 - \nu) - 2\Lambda\nu^o)b_k r_k - (2B\gamma_1 + \Lambda(1 + \gamma_2))b_j \epsilon_{jk} r_k] \left(\frac{r_i \epsilon_{jn} r_n + r_j \epsilon_{in} r_n}{r^2} \right) \right\} \quad (\text{S53})$$

Throughout, the qualitatively new terms introduced by Λ and Γ are the terms proportional to $b_m r_m$ in the trace and antisymmetric parts of the stress and strain, as well as the terms proportional to $b_j \epsilon_{jk} r_k$ in the symmetric traceless symmetric part of the stress and strain.

E. Local dilations and point torques

We now address defects with local dilations and torques at their core. Unlike disclinations and dislocations, which require that the displacement field to be multivalued, local dilations and torques describe properties of the core itself that are felt at large distances. An interstitial refers to the change in area of the core, characterized by a quantity Ω

$$\Omega = \oint_{\gamma} u_i \epsilon_{ij} dr_j. \quad (\text{S54})$$

Similarly, we may define the circulation φ of the displacement field about the core:

$$\varphi = \oint_{\gamma} u_i dr_i \quad (\text{S55})$$

In differential form, Eqs. (S54-S55) read:

$$\partial_i u_i(\mathbf{r}) = \Omega \delta(\mathbf{r}) \quad (\text{S56})$$

$$\partial_i \epsilon_{ij} u_j(\mathbf{r}) = \varphi \delta(\mathbf{r}) \quad (\text{S57})$$

whose solution is

$$u_i(\mathbf{r}) = \frac{\Omega}{2\pi} \frac{r_i}{r^2} + \frac{\varphi}{2\pi} \epsilon_{ij} \frac{r_j}{r^2} \quad (\text{S58})$$

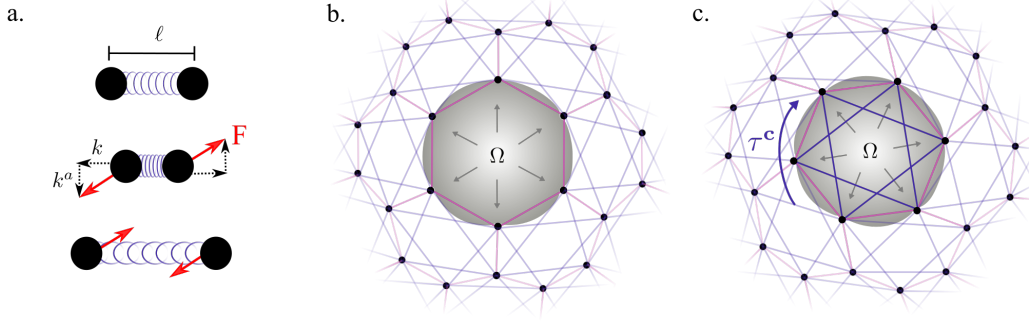


Fig. S1. **Generalized Hookean springs and point torques.** **a.** The generalized Hookean spring described in Eq. (S86). When compressed or elongated, the spring exhibits a pair of equal and opposite forces, whose magnitude F is proportional to the spring's change in length. The radial component of the force is proportional to the spring constant k and the transverse component is proportional to k^a . The transverse component results in a nonzero net torque. **b-c.** A microscopic point dilation Ω is induced by an expanding diaphragm (grey) in a lattice of active springs. In **b**, the next-nearest-neighbor springs crossing the diaphragm are removed, and in **c** the next-nearest-neighbor springs are kept in place. As a result, the torque τ^c at the center of the point defect is greater in **c** than in **b**.

The gradient of Eq. (S58) is given by

$$\partial_i u_j(\mathbf{r}) = \frac{\Omega}{2\pi r^2} \left(\frac{2r_i r_j}{r^2} - \delta_{ij} \right) + \frac{\varphi}{2\pi r^2} \left(\frac{r_i \epsilon_{jk} r_k + r_j \epsilon_{ik} r_k}{r^2} \right) \quad (\text{S59})$$

Due to Eq. (S56) and Eq. (S57), $\partial_i u_j$ in Eq. (S59) consists entirely of shear for $\mathbf{r} \neq 0$. Consequently, the stress corresponding to Eq. (S59) also consists entirely of shear:

$$\sigma_{ij}(\mathbf{r}) = \left(\frac{\mu\Omega - K^o\varphi}{2\pi r^2} \right) \left(\frac{2r_i r_j}{r^2} - \delta_{ij} \right) + \left(\frac{\varphi\mu + K^o\Omega}{2\pi r^2} \right) \left(\frac{r_i \epsilon_{jk} r_k + r_j \epsilon_{ik} r_k}{r^2} \right) \quad (\text{S60})$$

Notice that $\partial_i \sigma_{ij}(\mathbf{r}) = 0$ and $\epsilon_{ij} \sigma_{ij}(\mathbf{r}) = 0$ for all $\mathbf{r} \neq 0$. Using Eq. (S19), we find that Eq. (S60) captures the response to a point torque at $\mathbf{r} = 0$ whose magnitude is given by

$$\tau^c = \varphi\mu + K^o\Omega \quad (\text{S61})$$

Hence, we find that the strain field due to a defect depends both on the volume change Ω of the core and the torque τ^c provided by the core. In standard isotropic elasticity, Eq. (S61) implies that $\varphi = 0$, and hence Eq. (S58) yields the familiar strain distribution about an interstitial. When $\mu = 0$ and $K^o \neq 0$, Eq. (S61) implies that the core of a defect must experience a volume change when τ^c is nonzero in order to be mechanically stable.

In Sections S2B and S2C, we obtained the solutions for the disclination and dislocation for $\Omega = 0$ and $\tau^c = 0$. However, whenever angular momentum conservation is violated, a nonzero τ^c cannot be excluded on the basis of symmetry. In order to adjust the solutions in Sections S2B and S2C for nonzero τ^c and Ω , one need only solve Eq. (S61) for φ and then add Eq. (S58) and Eq. (S60) to the displacement and stress, respectively. For the disclination, in order to maintain stress free boundary conditions one need adjust

$$R_1 = R \exp \left\{ \frac{3[(\mu^2 + (K^o)^2)\Omega - K^o\tau^c]}{\mu B(1-\nu)sR^2} - \frac{1}{2} \right\} \quad (\text{S62})$$

$$R_2 = R \exp \left\{ \frac{3\tau^c}{B(1-\nu)sR^2} - \frac{1}{2} \right\} \quad (\text{S63})$$

Finally, we note that τ^c and Ω are contingent on the microscopic details of the topological defect. As an illustration, Fig. (S1) shows an inclusion in a lattice composed of bonds that exert torques when stretched or elongated, as described in Eq. (S86). In panel b, the next-nearest-neighbor springs are removed, while in panel c the next nearest neighbor springs are retained. Since each spring exerts a torque when elongated, the torque at the core will be greater in panel c than in panel b. This difference depends on the details of the microscopic construction and therefore must be provided phenomenologically.

S3. AIRY STRESS FUNCTION

Isotropic 2D elasticity is often simplified by the introduction of an Airy stress function [17, 61]. When $A = \Gamma = 0$, the stress tensor σ_{ij} is symmetric. Therefore, when the system is force balanced (i.e. $\partial_i \sigma_{ij} = 0$), we may write the stress as $\sigma_{ij} = \epsilon_{jk} \epsilon_{il} \partial_k \partial_l \chi$, where χ is the Airy stress function. Moreover, when $\Lambda = 0$, an invertible relationship exists between the symmetric stress σ_{ij} and the symmetric strain $u_{ij}^s = (\partial_i u_j + \partial_j u_i)/2$ given by:

$$u_{ij}^s = \frac{1}{E} \left\{ (1 - \nu) \delta_{ij} \delta_{mn} + (1 + \nu) (\delta_{im} \delta_{jn} + \delta_{in} \delta_{jm} - \delta_{ij} \delta_{mn}) - \frac{K^o}{\mu} (1 + \nu) E_{ijmn} \right\} \sigma_{mn} \quad (\text{S64})$$

where E is the Young's modulus generalized to include K^o :

$$E = \frac{4B[\mu^2 + (K^o)^2]}{\mu(B + \mu) + (K^o)^2} \quad (\text{S65})$$

Next, we utilize the differential versions of Eq. (S24) and Eq. (S35)

$$\epsilon_{ij} \partial_i \partial_j u_k = \sum_{\alpha} b_k^{\alpha} \delta(\mathbf{r} - \mathbf{r}^{\alpha}) \quad (\text{S66})$$

$$\epsilon_{ij} \partial_i \partial_j \epsilon_{lk} \partial_l u_k = \frac{2\pi}{3} \sum_{\alpha} s^{\alpha} \delta(\mathbf{r} - \mathbf{r}^{\alpha}) \quad (\text{S67})$$

where b_i^{α} and s^{α} are the charges associated with a defect at point \mathbf{r}^{α} . Hence, by evaluating $\partial_k \epsilon_{ki} \partial_l \epsilon_{lk} u_{ij}^s$, we obtain an expression identical in form to that of standard isotropic 2D elasticity:

$$\Delta^2 \chi = E s(\mathbf{r}) \quad (\text{S68})$$

where

$$s(\mathbf{r}) = \sum_{\alpha} \left[\frac{\pi}{3} s^{\alpha} + b_i^{\alpha} \epsilon_{ij} \partial_j \right] \delta(\mathbf{r} - \mathbf{r}^{\alpha}) \quad (\text{S69})$$

is the defect density. For a single disclination at the origin, we obtain $\Delta^2 \chi = E \pi s \delta(\mathbf{r})/3$, which yields a stress:

$$\sigma_{ij} = \frac{sE}{12} \left[\frac{\epsilon_{il} \epsilon_{jk} r_l r_k}{r^2} + \log(r) \right] \quad (\text{S70})$$

which agrees with Eq. (S31) upon setting $A = 0$ and using $E = 2B(1 - \nu)$. Similarly, for a single dislocation, we solve $\Delta^2 \chi = E b_i \partial_i \delta(\mathbf{x})$ to obtain

$$\sigma_{ij} = \frac{E}{4\pi r^2} \left[r_m \epsilon_{mn} b_n \delta_{ij} - b_k r_k \left(\frac{r_i \epsilon_{jm} r_m + r_j \epsilon_{im} r_m}{r^2} \right) \right], \quad (\text{S71})$$

in agreement with Eq. (S40) with $A \rightarrow 0$.

S4. DISLOCATION INTERACTION

A. Peach-Koehler Force

Here we provide a derivation of the Peach-Koehler formula in two dimensions with special attention to the fact that $\sigma_{ij}(\mathbf{r})$ need not be symmetric. Suppose that an isolated dislocation with Burgers vector b_i is subjected to an external stress field $\sigma_{ij}^{(\text{ext})}$ satisfying $\partial_i \sigma_{ij}^{(\text{ext})} = 0$. We seek to compute the work δW associated with moving the location of the defect from the point \mathbf{r}^0 to $\delta \mathbf{r} + \mathbf{r}^0$. The work done by the external stress is:

$$\delta W = - \int \left(\sigma_{ij}^{(\text{ext})} \partial_i \delta u_j \right) dA \quad (\text{S72})$$

$$= - \delta \int \left(\sigma_{ij}^{(\text{ext})} \partial_i u_j \right) dA \quad (\text{S73})$$

$$= - \delta \int \partial_i \left(\sigma_{ij}^{(\text{ext})} u_j \right) dA \quad (\text{S74})$$

where u_i is the displacement field associated with the dislocation. The δ indicates the change associated with the motion of the dislocation. Between Eq. (S72) and Eq. (S73), we used the fact that $\sigma_{ij}^{(\text{ext})}$ is the stress field due to an external source and therefore does not depend on the location of the dislocation. In the second step we used the fact that $\partial_i \sigma_{ij}^{(\text{ext})} = 0$. Next, let $y_i(\gamma) = r_i^0 + \gamma \delta r_i$ for $\gamma \in (0, \infty)$. Without loss of generality, we may choose y_i to be the line along which u_i experiences a discontinuity:

$$\lim_{\epsilon \rightarrow 0} [u_i(\mathbf{y} + \epsilon \hat{\mathbf{n}}) - u_i(\mathbf{y} - \epsilon \hat{\mathbf{n}})] = b_i \quad (\text{S75})$$

where $\hat{n}_i = \epsilon_{ij} \delta r_j / \delta r$ is normal to $dy_i / d\gamma$. We may apply Stokes' theorem to Eq. (S74) while treating $y_i(\gamma)$ as a two-sided boundary

$$\delta W = - \left[\lim_{\epsilon \rightarrow 0} \int_a^\infty \hat{n}_i [\sigma_{ij}^{(\text{ext})} u_j]_{\mathbf{y}-\epsilon \hat{\mathbf{n}}}^{\mathbf{y}+\epsilon \hat{\mathbf{n}}} d\gamma \right]_{a=0}^{a=1} \quad (\text{S76})$$

$$= - b_j \delta r \left[\int_a^\infty \hat{n}_i \sigma_{ij}^{(\text{ext})} d\gamma \right]_{a=0}^{a=1} \quad (\text{S77})$$

$$= b_j \delta r \hat{n}_i \sigma_{ij}^{(\text{ext})} \quad (\text{S78})$$

$$= b_j \epsilon_{im} \delta r_m \sigma_{ij}^{(\text{ext})} \quad (\text{S79})$$

Hence, we may express the work as $\delta W = \delta r_m f_m$ where f_m is the effective force on the dislocation, known as the Peach-Koehler force. Comparing with Eq. (S79), we obtain:

$$f_m = \epsilon_{mi} \sigma_{ij}^{(e)} b_j \quad (\text{S80})$$

Notice first that the Peach-Koehler force is agnostic to the elasticity of the solid and relies only on the expression for the virtual work and the definition of a dislocation. Secondly, the Peach-Koehler force is conservative in the sense that its curl vanishes:

$$\partial_k \epsilon_{km} f_m = -\partial_k \sigma_{kj}^{(\text{ext})} b_j = 0 \quad (\text{S81})$$

where we have used the assumption that $\partial_i \sigma_{ij}^{(\text{ext})} = 0$.

Finally, we note that Eq. (S80) does not directly predict the motion of the dislocation. For instance, the quantity $f_m \delta r_m$ yields the work done when δr is small but still larger than the microscopic lattice spacing. However forces associated with local bond rearrangements that are contingent on the microscopic structure of the dislocation can play a role in the dislocation motion. For example, such microscopic forces can constrain the dislocation to move along its glide plane [2, 17]. In this case, the dislocation motion in 2D is given by the projection of the Peach-Koehler force along the Burger's vector.

B. Non-reciprocal interactions

We now compute the interaction between two dislocations. Suppose a dislocation with Burger's vector b_i is located at the origin and a dislocation with Burger's vector d_i is located at point r_i . The force on d_i due to b_i is given by:

$$f_m = \epsilon_{mi} \sigma_{ij}^{(b)} d_j = \frac{(1-\nu)}{2\pi r^2} \left\{ B \left[r_k \epsilon_{kn} b_n \epsilon_{mj} d_j + r_k \epsilon_{ki} d_i \epsilon_{mk} b_k + r_m b_i d_j \left(\frac{2r_i r_j}{r^2} - \delta_{ij} \right) \right] + A \left[r_m d_i \epsilon_{ij} b_j + \epsilon_{mn} r_n b_i d_j \left(\frac{2r_i r_j}{r^2} - \delta_{ij} \right) \right] \right\} \quad (\text{S82})$$

Notice that when $A \rightarrow 0$, we recover the usual defect interaction, which is notably symmetric under $b_i \leftrightarrow d_i$ and $r_i \rightarrow -r_i$. When A is nonzero, the Peach-Koehler force violates this symmetry and one therefore obtains:

$$f_m^{b \rightarrow d} + f_m^{d \rightarrow b} = \frac{(1-\nu)}{\pi r^2} A r_m d_i \epsilon_{ij} b_j \quad (\text{S83})$$

as given in Eq. (11) of the main text. When Γ and Λ are nonzero, the antisymmetric part of the Peach-Koehler force generalizes to

$$f_m^{b \rightarrow d} + f_m^{d \rightarrow b} = \frac{2}{\pi r^2} d_i \epsilon_{ij} b_j r_m \frac{(A - \Lambda)[\mu^2 + (K^o)^2] + 2K^o(B\Gamma - A\Lambda)}{(B + \mu)(\mu + \Gamma) + (A + K^o)(K^o - \Lambda)} \quad (\text{S84})$$

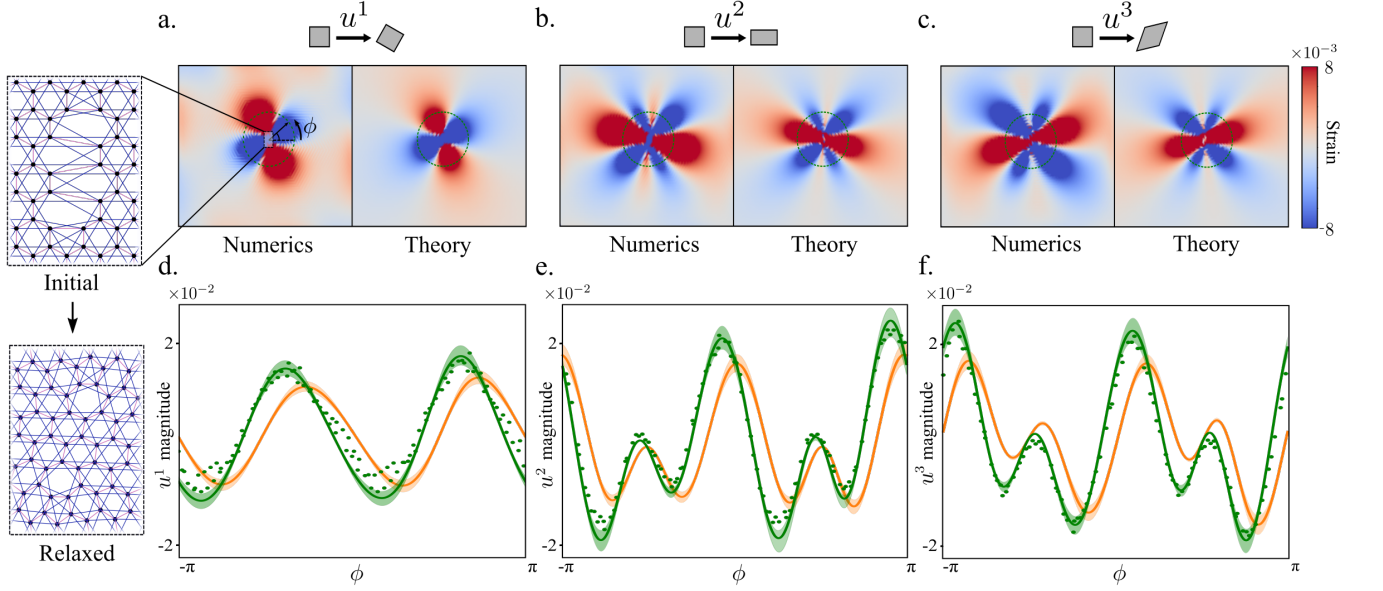


Fig. S2. **Strain field of a dislocation pair.** **a-c.** The distribution of rotation (u^1), shear 1 (u^2), and shear 2 (u^3) surrounding a pair of dislocations in a non-reciprocal solid with $\nu = 0.8$ and $\nu^\circ = -0.88$. The right panels visualize the continuum theory while the left panel is the result of numerics. The inset to panel (a) renders the individual masses and bonds comprising the dislocation pair before (top) and after (bottom) relaxation. **d-f.** We quantitatively compare numerics and experiments by sampling the strain (green dots) at points between 8.0 and 9.2 lattice spacings from the center. The green line is the theoretical curve with $\nu = 0.8$ and $\nu^\circ = -0.88$. The shaded background accounts in the variation in distance from the center. The orange lines, provided for reference, are theoretical curves for a passive solid with $\nu = 0.8$ and $\nu^\circ = 0$. We note that the dilation (u^0) is too small for numerical validation.

Notice that Eq. (S84) indicates that there is a net force on the dislocation pair pointing along their relative separation vector. Moreover, the strength of the force is proportional the cross product of the two Burgers vectors.

In Fig. 3 of the main text, we illustrate the interaction between two dislocations with parallel glide planes. For simplicity, let us take $\mathbf{b} = b\hat{\mathbf{x}}$ and $\mathbf{d} = d\hat{\mathbf{x}}$. Then the force f on the relative coordinate r_x is given by:

$$f(r_x) = \frac{(1-\nu)bd}{\pi r^4} (r_x^2 - r_y^2)(Br_x + Ar_y) \quad (\text{S85})$$

Notice, that $f(r_x) = 0$ for $r_x = \pm r_y$ and $r_x = -(A/B)r_y$. For the antiparallel defects in Fig. 3, we take $bd < 0$. In this case, the solutions $r_x = \pm r_y$ are stable for $A < B$ and the solutions $r_x = r_y$ and $r_x = -(A/B)r_y$ are stable for $A > B$. In the limit $A/B \rightarrow \infty$, only one stable configuration remains. Notice that when $bd > 0$, the stability of each solution is inverted.

S5. NUMERICS AND MICROSCOPIC MODEL

In this section we discuss the microscopic model used to validate the analytical calculations of the strain field. As presented in Ref. [66], we use a mass spring network in which the generalized Hookean springs in which the force F_i exerted by mass 1 on mass 2 is given by:

$$F_i(\mathbf{r}) = -(k\hat{r}_i + k^a\epsilon_{ij}\hat{r}_j)(r - \ell) \quad (\text{S86})$$

where \mathbf{r} is the vector pointing from mass 1 to mass 2. As shown in Fig. S1a, ℓ is the rest length of the bond, k is the standard Hookean spring constant that acts radially along the bonds and k^a is an active spring constant that provides a force transverse to the bonds. We use a honeycomb lattice with nearest-neighbor and next-nearest-neighbor bonds. Such a lattice permits an analytical coarsegraining thereby allowing the expression of macroscopic elastic coefficients in terms of microscopic parameters [66]. Specifically, we have

$$B = \frac{k_{\text{NN}} + 6k_{\text{NNN}}}{2\sqrt{3}} \quad A = \frac{k_{\text{NN}}^a + 6k_{\text{NNN}}^a}{2\sqrt{3}} \quad \mu = \frac{\sqrt{3}k_{\text{NNN}}}{2} \quad K^\circ = \frac{\sqrt{3}k_{\text{NNN}}^a}{2} \quad (\text{S87})$$

where the subscripts NN and NNN denote the nearest-neighbor and next-nearest-neighbor parameters, respectively.

For the data shown in Fig. 1, we simulate a 60×60 unit cell rectangle with free boundary conditions. As shown in the inset of Fig. S2a, we introduce a dislocation pair vertically separated by four unit cells by removing a column of 8 particles from the center of the lattice and locally reassigning bonds. We then allow the lattice to relax under first order dynamics, integrated using second-order Runge-Kutta. Once the lattice equilibrates, we compute the strain at each node by performing a linear regression from an undeformed template hexagon to the hexagon defined by next-nearest-neighbor connections. For the data shown in Fig. 1 and Fig. S2, we have $k_{\text{NN}} = 0.92$, $k_{\text{NN}}^a = 0.39$, $k_{\text{NNN}} = 0.027$, and $k_{\text{NNN}}^a = 0.012$ which corresponds to $\nu = 0.8$ and $\nu^o = -0.88$.

The theoretical curves in Fig. 1b are produced via suppositions of the exact continuum solutions in Eq. (S39). Insight into the form of the curves can be gained by computing the approximate strain field to leading order in the separation between the dislocations, i.e. a dipole approximation. Consider a pair of dislocations with Burgers vectors $\mathbf{b}_{\pm} = \pm b \hat{\mathbf{x}}$ at locations $(0, \pm \delta r/2)$. When $\nu^o = 0$, the shear strain \tilde{u}_{ij} to leading order in δr is given by:

$$\tilde{u}_{ij} \propto \frac{b\delta r}{2r^2} \begin{pmatrix} \cos 2\phi + \cos 4\phi & \sin 2\phi + \sin 4\phi \\ \sin 2\phi + \sin 4\phi & -\cos 2\phi - \cos 4\phi \end{pmatrix} \quad (\text{S88})$$

where we have set aside constant prefactors. Hence, we have

$$u^2 = \tau_{ij}^2 \tilde{u}_{ij} \propto \frac{b\delta r}{r^2} (\cos 2\phi + \cos 4\phi) \quad (\text{S89})$$

$$u^3 = \tau_{ij}^3 \tilde{u}_{ij} \propto \frac{b\delta r}{r^2} (\sin 2\phi + \sin 4\phi) \quad (\text{S90})$$

Finally, the angle α is defined as

$$Re^{2i\alpha} = u^2 + iu^3 \quad (\text{S91})$$

with a positive amplitude R that represents the total magnitude of the shear strain. We find

$$\alpha = \frac{3}{2}\phi - \frac{\pi}{4}(1 - \text{sgn}(\cos \phi)) \quad (\text{S92})$$

Physically, the angle α specifies the axis of elongation for the local shear and is therefore periodic modulo π . Notice that α contains discontinuities at $\phi = \pm\pi/2$. However, the amplitude $R \propto \cos^2(\phi)/r^2$ vanishes at these angles, so the physical strain field is continuous. Finally, when ν^o is nonzero, the expression for α simply receives an additive correction $\delta\alpha = -\arctan[2\nu^o/(1+\nu)]/2$ to yields:

$$\alpha = \frac{3}{2}\phi - \frac{\pi}{4}[1 - \text{sgn}(\cos \phi)] - \frac{1}{2} \arctan\left(\frac{2\nu^o}{1+\nu}\right) \quad (\text{S93})$$

Equation (S93) is the dipole approximation for the theoretical curve shown in Fig. 1b and is the analogue of Eqs. (8-9) for the disclination and dislocation in the main text.

-
- [1] Nelson, D. R. *Defects and geometry in condensed matter physics* (Cambridge University Press, Cambridge ; New York, 2002).
 - [2] Weertman, J. *Elementary dislocation theory*. Macmillan series in materials science (Macmillan, New York, 1964).
 - [3] Chaikin, P. M. *Principles of condensed matter physics* (Cambridge University Press, Cambridge ; New York, NY, USA, 1995).
 - [4] Paulose, J., Chen, B. G.-g. & Vitelli, V. Topological modes bound to dislocations in mechanical metamaterials. *Nat Phys* **11**, 153–156 (2015).
 - [5] Mietke, A. & Dunkel, J. Anyonic defect braiding and spontaneous chiral symmetry breaking in dihedral liquid crystals. *arXiv:2011.04648* (2020).
 - [6] Pretko, M. & Radzihovsky, L. Fracton-elasticity duality. *Phys. Rev. Lett.* **120**, 195301 (2018).
 - [7] Duclos, G. *et al.* Topological structure and dynamics of three-dimensional active nematics. *Science* **367**, 1120–1124 (2020).
 - [8] Shankar, S., Souslov, A., Bowick, M. J., Marchetti, M. C. & Vitelli, V. Topological active matter. *arXiv:2010.00364* (2020).
 - [9] Colen, J. *et al.* Machine learning active-nematic hydrodynamics. *arXiv:2006.13203* (2020).

- [10] Vafa, F., Bowick, M. J., Marchetti, M. C. & Shraiman, B. I. Multi-defect dynamics in active nematics. *arXiv:2007.02947* (2020).
- [11] Pearce, D. J. G., Gat, S., Livne, G., Bernheim-Groswasser, A. & Kruse, K. Programming active metamaterials using topological defects. *arXiv:2010.13141* (2020).
- [12] Thijssen, K. & Doostmohammadi, A. Binding self-propelled topological defects in active turbulence. *Phys. Rev. Research* **2**, 042008 (2020).
- [13] Maitra, A., Lenz, M. & Voituriez, R. Chiral active hexatics: Giant number fluctuations, waves and destruction of order. *arXiv:2004.09115* (2020).
- [14] Gupta, R. K., Kant, R., Soni, H., Sood, A. K. & Ramaswamy, S. Active nonreciprocal attraction between motile particles in an elastic medium. *arXiv:2007.04860* (2020).
- [15] Kumar, N., Soni, H., Ramaswamy, S. & Sood, A. K. Flocking at a distance in active granular matter. *Nature Communications* **5**, 4688 (2014).
- [16] VanSaders, B. & Glotzer, S. C. Pinning dislocations in colloidal crystals with active particles that seek stacking faults. *Soft Matter* **16**, 4182–4191 (2020).
- [17] Landau, L. *et al.* *Theory of Elasticity*. Course of theoretical physics (Elsevier Science, 1986).
- [18] van Zuiden, B. C., Paulose, J., Irvine, W. T. M., Bartolo, D. & Vitelli, V. Spatiotemporal order and emergent edge currents in active spinner materials. *Proc. Natl. Acad. Sci. USA* **113**, 12919–12924 (2016).
- [19] Menzel, A. M. & Löwen, H. Traveling and resting crystals in active systems. *Phys. Rev. Lett.* **110**, 055702 (2013).
- [20] Menzel, A. M., Ohta, T. & Löwen, H. Active crystals and their stability. *Phys. Rev. E* **89**, 022301 (2014).
- [21] Heinonen, V. *et al.* Consistent hydrodynamics for phase field crystals. *Phys. Rev. Lett.* **116**, 024303 (2016).
- [22] Alaimo, F., Praetorius, S. & Voigt, A. A microscopic field theoretical approach for active systems. *New Journal of Physics* **18**, 083008 (2016).
- [23] Huang, Z.-F., Menzel, A. M. & Löwen, H. Dynamical crystallites of active chiral particles. *Phys. Rev. Lett.* **125**, 218002 (2020).
- [24] Fruchart, M., Hanai, R., Littlewood, P. B. & Vitelli, V. Phase transitions in non-reciprocal active systems. *arXiv:2003.13176* (2020).
- [25] Lahiri, R. & Ramaswamy, S. Are steadily moving crystals unstable? *Physical Review Letters* **79**, 1150–1153 (1997).
- [26] Nassar, H. *et al.* Nonreciprocity in acoustic and elastic materials. *Nature Reviews Materials* **5**, 667–685 (2020).
- [27] Achenbach, J. D. *Reciprocity in Elastodynamics* (Cambridge University Press, 2004).
- [28] Masoud, H. & Stone, H. A. The reciprocal theorem in fluid dynamics and transport phenomena. *Journal of Fluid Mechanics* **879** (2019).
- [29] De Groot, S. R. & Mazur, P. *Non-Equilibrium Thermodynamics (Dover Books on Physics)* (Dover Publications, 1962).
- [30] Durve, M., Saha, A. & Sayeed, A. Active particle condensation by non-reciprocal and time-delayed interactions. *The European Physical Journal E* **41**, – (2018).
- [31] Saha, S., Agudo-Canalejo, J. & Golestanian, R. Scalar active mixtures: The non-reciprocal cahn-hilliard model (2020). 2005.07101.
- [32] Saha, S., Ramaswamy, S. & Golestanian, R. Pairing, waltzing and scattering of chemotactic active colloids. *New Journal of Physics* **21**, 063006 (2019).
- [33] Loos, S. A. M., Hermann, S. M. & Klapp, S. H. L. Non-reciprocal hidden degrees of freedom: A unifying perspective on memory, feedback, and activity (2019). 1910.08372v1.
- [34] Loos, S. A. M. & Klapp, S. H. L. Thermodynamic implications of non-reciprocity (2020). 2008.00894v1.
- [35] You, Z., Baskaran, A. & Marchetti, M. C. Nonreciprocity as a generic route to traveling states (2020). 2005.07684.
- [36] Banerjee, D., Souslov, A., Abanov, A. G. & Vitelli, V. Odd viscosity in chiral active fluids. *Nature Communications* **8**, 1573 (2017).
- [37] Han, M. *et al.* Statistical mechanics of a chiral active fluid (2020). 2002.07679.
- [38] Khain, T., Scheibner, C. & Vitelli, V. Stokes flows in three-dimensional fluids with odd viscosity (2020). 2011.07681.
- [39] Souslov, A., Gromov, A. & Vitelli, V. Anisotropic odd viscosity via a time-modulated drive. *Phys. Rev. E* **101**, 052606 (2020).
- [40] Souslov, A., Dasbiswas, K., Fruchart, M., Vaikuntanathan, S. & Vitelli, V. Topological waves in fluids with odd viscosity. *Phys. Rev. Lett.* **122**, 128001 (2019).
- [41] Coulais, C., Sounas, D. & Alù, A. Static non-reciprocity in mechanical metamaterials. *Nature* **542**, 461 (2017).
- [42] Markovich, T. & Lubensky, T. C. Odd viscosity in active matter: microscopic origin and 3d effects (2020). 2006.05662.
- [43] Fleury, R., Sounas, D. L., Sieck, C. F., Haberman, M. R. & Alù, A. Sound isolation and giant linear nonreciprocity in a compact acoustic circulator. *Science (New York, N.Y.)* **343**, 516–9 (2014).
- [44] Brandenbourger, M., Locsin, X., Lerner, E. & Coulais, C. Non-reciprocal robotic metamaterials. *Nature Communications* **10**, 4608 (2019).
- [45] Ghatak, A., Brandenbourger, M., van Wezel, J. & Coulais, C. Observation of non-hermitian topology and its bulk-edge correspondence (2019). arXiv:1907.11619v1.
- [46] Lavergne, F. A., Wendehenne, H., Baeuerle, T. & Bechinger, C. Group formation and cohesion of active particles with visual perception-dependent motility. *Science* **364**, 70–74 (2019).
- [47] Bonilla, L. L. & Trenado, C. Contrarian compulsions produce exotic time-dependent flocking of active particles. *Physical Review E* **99**, 012612 (2019).
- [48] Dadhichi, L. P., Kethapelli, J., Chajwa, R., Ramaswamy, S. & Maitra, A. Nonmutual torques and the unimportance of motility for long-range order in two-dimensional flocks. *Physical Review E* **101**, 052601 (2020).

- [49] Agudo-Canalejo, J. & Golestanian, R. Active phase separation in mixtures of chemically interacting particles. *Physical Review Letters* **123**, 018101 (2019).
- [50] Kryuchkov, N. P., Ivlev, A. V. & Yurchenko, S. O. Dissipative phase transitions in systems with nonreciprocal effective interactions. *Soft Matter* **14**, 9720–9729 (2018).
- [51] Ivlev, A. V. *et al.* Statistical mechanics where Newton’s third law is broken. *Physical Review X* **5**, 011035 (2015).
- [52] Hong, H. & Strogatz, S. H. Kuramoto model of coupled oscillators with positive and negative coupling parameters: An example of conformist and contrarian oscillators. *Physical Review Letters* **106**, 054102 (2011).
- [53] Cavagna, A. *et al.* Nonsymmetric interactions trigger collective swings in globally ordered systems. *Phys. Rev. Lett.* **118**, 138003 (2017).
- [54] Hayashi, K. & ichi Sasa, S. The law of action and reaction for the effective force in a non-equilibrium colloidal system. *Journal of Physics: Condensed Matter* **18**, 2825–2836 (2006).
- [55] Bain, N. & Bartolo, D. Dynamic response and hydrodynamics of polarized crowds. *Science* **363**, 46–49 (2019).
- [56] Yan, J., Bae, S. C. & Granick, S. Rotating crystals of magnetic Janus colloids. *Soft Matter* **11**, 147–153 (2015).
- [57] Han, F. *et al.* Crossover from positive to negative optical torque in mesoscale optical matter. *Nature Communications* **9**, 4897 (2018).
- [58] Bertoldi, K., Vitelli, V., Christensen, J. & van Hecke, M. Flexible mechanical metamaterials. *Nature Reviews Materials* **2**, 17066 (2017).
- [59] Hexemer, A., Vitelli, V., Kramer, E. J. & Fredrickson, G. H. Monte carlo study of crystalline order and defects on weakly curved surfaces. *Phys. Rev. E* **76**, 051604 (2007).
- [60] Bowick, M. J. & Giomi, L. Two-dimensional matter: order, curvature and defects. *Advances in Physics* **58**, 449–563 (2009).
- [61] Nelson, D.R. & Peliti, L. Fluctuations in membranes with crystalline and hexatic order. *J. Phys. France* **48**, 1085–1092 (1987).
- [62] Zhang, G. & Nelson, D. Statistical mechanics of dislocation pileups. *Bulletin of the American Physical Society* **65** (2020).
- [63] Vitelli, V., Xu, N., Wyart, M., Liu, A. J. & Nagel, S. R. Heat transport in model jammed solids. *Phys. Rev. E* **81**, 021301 (2010).
- [64] Irvine, W. T. M., Vitelli, V. & Chaikin, P. M. Pleats in crystals on curved surfaces. *Nature* **468**, 947–951 (2010).
- [65] Moshe, M., Levin, I., Aharoni, H., Kupferman, R. & Sharon, E. Geometry and mechanics of two-dimensional defects in amorphous materials. *Proceedings of the National Academy of Sciences* **112**, 10873–10878 (2015).
- [66] Scheibner, C. *et al.* Odd elasticity. *Nature Physics* **16**, 475–480 (2020).
- [67] Scheibner, C., Irvine, W. T. M. & Vitelli, V. Non-hermitian band topology and skin modes in active elastic media. *Phys. Rev. Lett.* **125**, 118001 (2020).
- [68] Zhou, D. & Zhang, J. Non-hermitian topological metamaterials with odd elasticity. *Phys. Rev. Research* **2**, 023173 (2020).
- [69] Chen, Y., Li, X., Scheibner, C., Vitelli, V. & Huang, G. Self-sensing metamaterials with odd micropolarity. *arXiv:2009.07329* (2020).
- [70] Banerjee, D., Vitelli, V., Jülicher, F. & Surówka, P. Active viscoelasticity of odd materials (2020). 2002.12564.
- [71] Lakes, R. S. Physical meaning of elastic constants in cosserat, void, and microstretch elasticity. *Journal of Mechanics of Materials and Structures* **11**, 217–229 (2016).
- [72] Rueger, Z. & Lakes, R. S. Strong cosserat elasticity in a transversely isotropic polymer lattice. *Phys. Rev. Lett.* **120**, 065501 (2018).
- [73] Eringen, A. C. *Microcontinuum field theories* (Springer, New York, 1999).
- [74] Gromov, A. & Surówka, P. On duality between Cosserat elasticity and fractons. *SciPost Phys.* **8**, 65 (2020).
- [75] Maitra, A. & Ramaswamy, S. Oriented active solids. *Phys. Rev. Lett.* **123**, 238001 (2019).
- [76] Born, M. *Dynamical theory of crystal lattices*. The International series of monographs on physics (Clarendon Press, Oxford, 1954).
- [77] Vitelli, V., Lucks, J. B. & Nelson, D. R. Crystallography on curved surfaces. *Proceedings of the National Academy of Sciences* **103**, 12323–12328 (2006).
- [78] Thouless, D. J., Ao, P. & Niu, Q. Transverse force on a quantized vortex in a superfluid. *Phys. Rev. Lett.* **76**, 3758–3761 (1996).
- [79] Wiegmann, P. & Abanov, A. G. Anomalous hydrodynamics of two-dimensional vortex fluids. *Phys. Rev. Lett.* **113**, 034501 (2014).
- [80] Nguyen, D. X., Gromov, A. & Moroz, S. Fracton-elasticity duality of two-dimensional superfluid vortex crystals: defect interactions and quantum melting. *arXiv:2005.12317* (2020).
- [81] Bogatskiy, A. & Wiegmann, P. Edge wave and boundary vorticity layer of vortex matter. *arXiv:1812.00763* (2018).
- [82] Bogatskiy, A. Vortex flows on closed surfaces. *Journal of Physics A: Mathematical and Theoretical* **52**, 475501 (2019).
- [83] Moroz, S., Hoyos, C., Benzoni, C. & Son, D. T. Effective field theory of a vortex lattice in a bosonic superfluid. *SciPost Phys.* **5**, 39 (2018).
- [84] Turner, A. M., Vitelli, V. & Nelson, D. R. Vortices on curved surfaces. *Rev. Mod. Phys.* **82**, 1301–1348 (2010).
- [85] Gifford, S. A. & Baym, G. Dislocation-mediated melting in superfluid vortex lattices. *Phys. Rev. A* **78**, 043607 (2008).
- [86] Moroz, S. & Son, D. T. Bosonic superfluid on the lowest landau level. *Phys. Rev. Lett.* **122**, 235301 (2019).
- [87] Sonin, E. B. Vortex oscillations and hydrodynamics of rotating superfluids. *Rev. Mod. Phys.* **59**, 87–155 (1987).
- [88] Fetter, A. L. Rotating trapped bose-einstein condensates. *Rev. Mod. Phys.* **81**, 647–691 (2009).
- [89] Abo-Shaer, J. R., Raman, C., Vogels, J. M. & Ketterle, W. Observation of vortex lattices in bose-einstein condensates. *Science* **292**, 476–479 (2001).

- [90] Tkachenko, V. On vortex lattices. *Sov. Phys. JETP* **22**, 1282–1286 (1966).
- [91] Tkachenko, V. K. Elasticity of vortex lattices. *JETP* **29**, 945 (1969).
- [92] Tkachenko, V. Stability of vortex lattices. *Sov. Phys. JETP* **23**, 1049–1056 (1966).
- [93] Marchetti, M. C. & Radzihovsky, L. Interstitials, vacancies, and dislocations in flux-line lattices: A theory of vortex crystals, supersolids, and liquids. *Phys. Rev. B* **59**, 12001–12020 (1999).
- [94] Šášik, R. & Stroud, D. Calculation of the shear modulus of a two-dimensional vortex lattice. *Phys. Rev. B* **49**, 16074–16077 (1994).
- [95] Hu, J. & MacDonald, A. H. Two-dimensional vortex lattice melting. *Phys. Rev. Lett.* **71**, 432–435 (1993).
- [96] Fisher, D. S. Flux-lattice melting in thin-film superconductors. *Phys. Rev. B* **22**, 1190–1199 (1980).
- [97] Abrikosov, A., Kemoklidze, M. & Khalatnikov, I. Hydrodynamic theory of collective oscillations of vortices in type II superconductors. *JETP* **21**, 506 (1965).
- [98] Abrikosov, A. A. On the magnetic properties of superconductors of the second group. *Sov. Phys. JETP* **5**, 1174–1182 (1957).
- [99] Bardeen, J. & Stephen, M. J. Theory of the motion of vortices in superconductors. *Phys. Rev.* **140**, A1197–A1207 (1965).
- [100] Rajeswari, J. *et al.* Filming the formation and fluctuation of skyrmion domains by cryo-lorentz transmission electron microscopy. *Proceedings of the National Academy of Sciences* **112**, 14212–14217 (2015).
- [101] Brun, M., Jones, I. S. & Movchan, A. B. Vortex-type elastic structured media and dynamic shielding. *Proceedings of the Royal Society A: Mathematical, Physical and Engineering Sciences* **468**, 3027–3046 (2012).
- [102] Carta, G., Jones, I. S., Movchan, N. V., Movchan, A. B. & Nieves, M. J. “deflecting elastic prism” and unidirectional localisation for waves in chiral elastic systems. *Scientific Reports* **7**, 26 (2017).
- [103] Carta, G., Brun, M., Movchan, A., Movchan, N. & Jones, I. Dispersion properties of vortex-type monatomic lattices. *International Journal of Solids and Structures* **51**, 2213 – 2225 (2014).
- [104] Benzoni, C., Jeevanesan, B. & Moroz, S. Rayleigh edge waves in two-dimensional chiral crystals. *arXiv:2004.09517* (2020).
- [105] Hassanpour, S. Dynamics of gyroelastic continua (2014).
- [106] Nash, L. M. *et al.* Topological mechanics of gyroscopic metamaterials. *Proc. Natl. Acad. Sci. USA* **112**, 14495–500 (2015).
- [107] Wang, P., Lu, L. & Bertoldi, K. Topological Phononic Crystals with One-Way Elastic Edge Waves. *Physical review letters* **115**, 104302 (2015).
- [108] Zhao, Y., Zhou, X. & Huang, G. Non-reciprocal rayleigh waves in elastic gyroscopic medium. *Journal of the Mechanics and Physics of Solids* **143**, 104065 (2020).
- [109] Vitelli, V. & Turner, A. M. Anomalous coupling between topological defects and curvature. *Phys. Rev. Lett.* **93**, 215301 (2004).
- [110] Here we use the convention that the force is the divergence on the first index of the stress $f_j = \partial_i \sigma_{ij}$. If the convention $f_i = \partial_j \sigma_{ij}$ is used, then the condition for Maxwell-Betti reciprocity reads $C_{ijmn} = C_{jinm}$.